

# Porous carbon nanosheets with precisely tunable thickness and selective CO<sub>2</sub> adsorption properties

Guang-Ping Hao, Zhen-Yu Jin, Qiang Sun, Xiang-Qian Zhang, Jin-Tao Zhang, and An-Hui

Lu\*

State Key Laboratory of Fine Chemicals, School of Chemical Engineering, Dalian University  
of Technology, Dalian 116024, P. R. China

E-mail: anhuilu@dlut.edu.cn

**Heat of CO<sub>2</sub> adsorption calculation.**<sup>1,2</sup> The enthalpy of CO<sub>2</sub> adsorption onto the PCNs was calculated using the Clausius-Clapeyron equation:

$$\ln\left(\frac{P_1}{P_2}\right) = Q_{st} \times \frac{T_2 - T_1}{R \times T_1 \times T_2} \quad (\text{I})$$

where  $P_i$  = pressure for isotherm  $i$ ;  $T_i$  = temperature for isotherm  $i$ ;  $R = 8.315 \text{ J K}^{-1} \text{ mol}^{-1}$ ; which can be used to calculate the enthalpy of adsorption of a gas as a function of the quantity of gas adsorbed. Pressure as a function of the amount of CO<sub>2</sub> adsorbed was determined by the Toth model for the isotherms (Figure 5a and Figure S8a).

$$C = \frac{C_m \times B^{(1/t)} P}{(1 + B \times P)^{1/t}} \quad (\text{II})$$

where  $C$  = moles adsorbed;  $C_m$  = moles adsorbed at saturation;  $P$  = pressure;  $B$  and  $t$  = constants; which can be used to calculate the pressure,  $P$ . Then, we can get the adsorption data, which were filled into equation (I) giving the  $Q_{st}$ .

**Table S1.** The structural parameters of the PCNs

Sample	$S_{\text{BET}}$ ( $\text{m}^2 \text{g}^{-1}$ )	$V_{\text{total}}$ ( $\text{cm}^3 \text{g}^{-1}$ )	$V_{\text{micro}}$ ( $\text{cm}^3 \text{g}^{-1}$ )	Thickness (nm)
PCN-9.9	350	0.45	0.12	$9.9 \pm 1$
PCN-17	576	0.33	0.23	$17 \pm 2$
PCN-71	610	0.31	0.26	$71 \pm 3$

**Table S2.** CO<sub>2</sub> uptake comparison of various porous materials <sup>a</sup>

Materials	CO <sub>2</sub> uptake ( $\text{mmol g}^{-1}$ )		Ref.
	1 bar	0.04 bar	
PCN-19	2.02	0.33	This study
PCN-17	2.36	0.34	
PCN-71	2.88	0.41	
commercial activated carbons, e.g., Norit R1, Extra, BPL, Maxsorb, A10 fiber	< 2		3
activated anthracites	1.49		4
ammoniated carbons	2.2		5
activated carbon ( $S_{\text{BET}}$ : $2829 \text{ m}^2 \text{g}^{-1}$ )	2.92		6
activated urea-formaldehyde resin based carbons	1.86		7
KOH-activated graphite nanofibers	1.35		8
KOH-activated polyanilines-derived carbons	4.3		9
KOH-activated templated carbons	3.4		10
soft-templated mesoporous carbons	1.49		11
hard-templated CMK-3	1.7		12
N-doped porous carbon monolith	3.13		13
HCM-1	2.6		14
KOH activated graphenes	< 4 at 0 °C		15
ZIF-81	2.2		16,17
ZIF-82	2.2		
ZIF-95	< 1		
CPF-6 (with 67% of N-donor sites)	4.5 at 0 °C		18
bio-MOF-11	4.1		19

<sup>a</sup> Unless otherwise specified, the CO<sub>2</sub> uptake listed were measured at 25 °C.

**Table S3.** Surface composition of PCN-17 and PCN-71 based on XPS results

	C (at%)	O (at%)	N (at%)
PCN-17	94.42	4.37	1.21
PCN-71	94.62	4.13	1.25

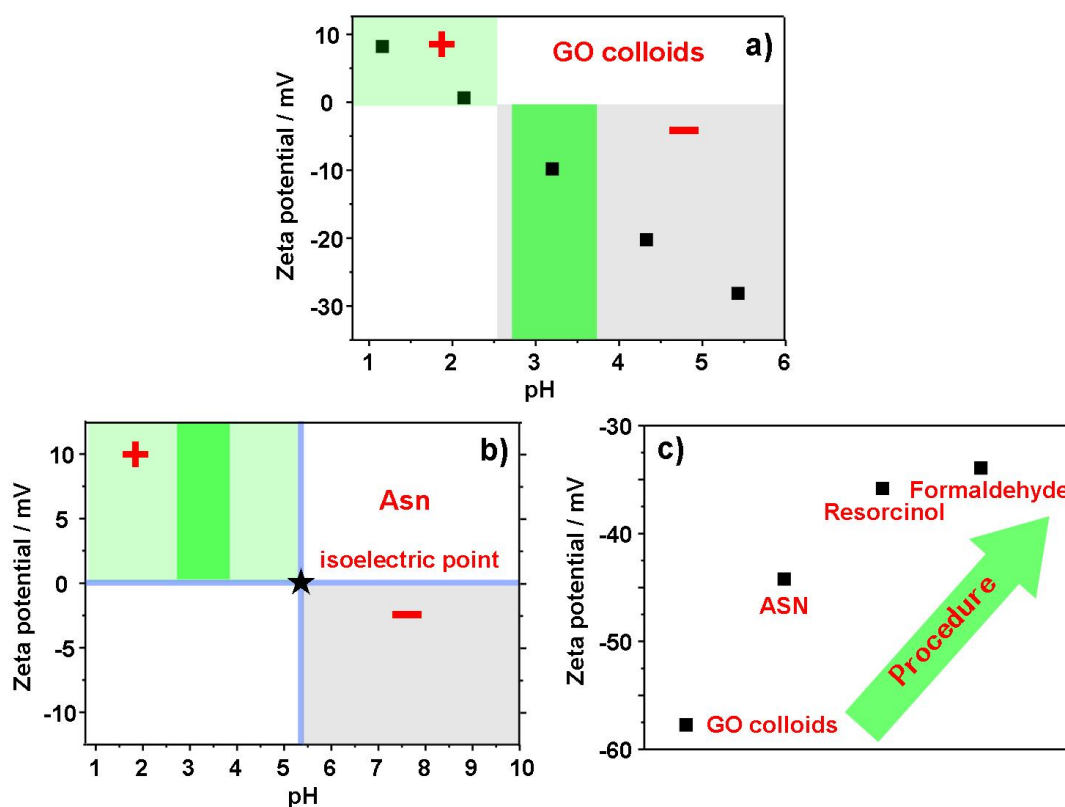


**Fig. S1** Charge properties of the synthesis solution. a, b) Zeta potential of GO (concentration of 0.05 mL g<sup>-1</sup>) and asparagine (9 mg mL<sup>-1</sup>) as a function of pH, in aqueous dispersions. The highlighted green parts in a) & b) show the working area of the synthesis; c) the zeta potential changing as the addition sequence of the reactants.

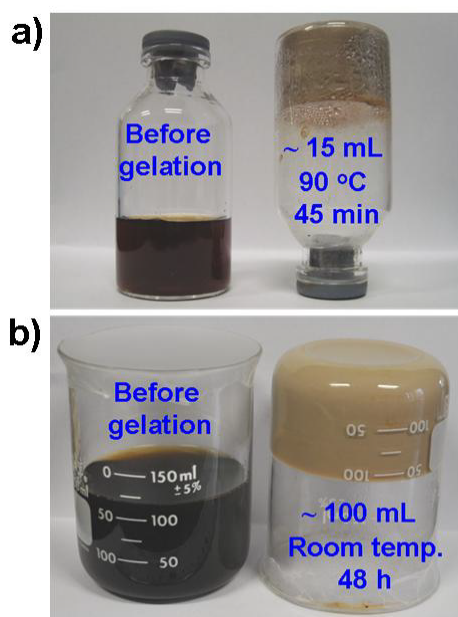


**Fig. S2** The phenomena of the co-polymerization under different conditions: a) photographs taken at the start point (left) and 45 min (right) aging at 90 °C; b) photographs taken at the start point (left) and 48 h (right) at room temperature.

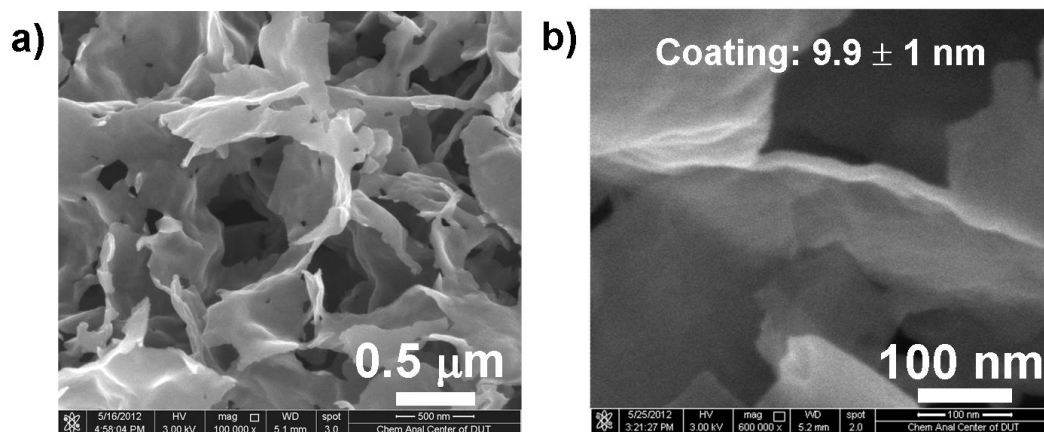


**Fig. S3** The FE-SEM images of sample PCN-9.9: a) with a low magnification, b) with a high magnification. This sample was obtained through freeze drying. As shown, the thickness of the carbon nanosheet is ca. 20 nm (on each side, the carbon coating is about 9.9 nm).

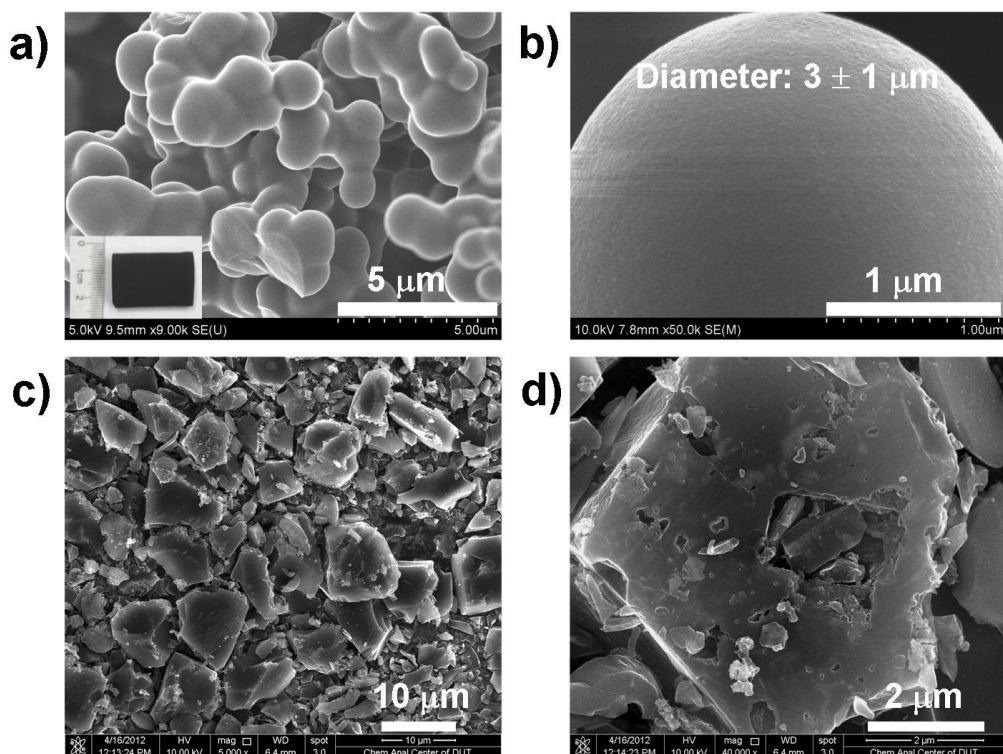


**Fig. S4** a, b) The FE-SEM images with a low magnification and high magnification of the control sample obtained without using GO. The average size of the sample prepared without GO is *ca.* 3 μm. c, d) The FE-SEM images with a low magnification and high magnification of a commercial activated carbon. As shown, the average size of the activated carbon particle is *ca.* 10 μm.

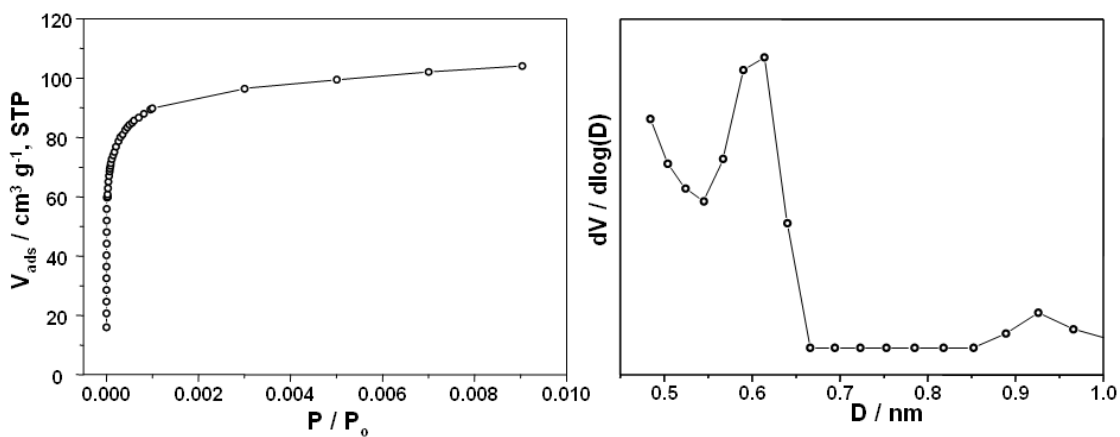


**Fig. S5** a) The low pressure range of the N<sub>2</sub> adsorption isotherm of PCN-17 at -196 °C and b) the corresponding PSD calculated by QSDFT method using Quantachrome Autosorb iQ physisorption analyzer.

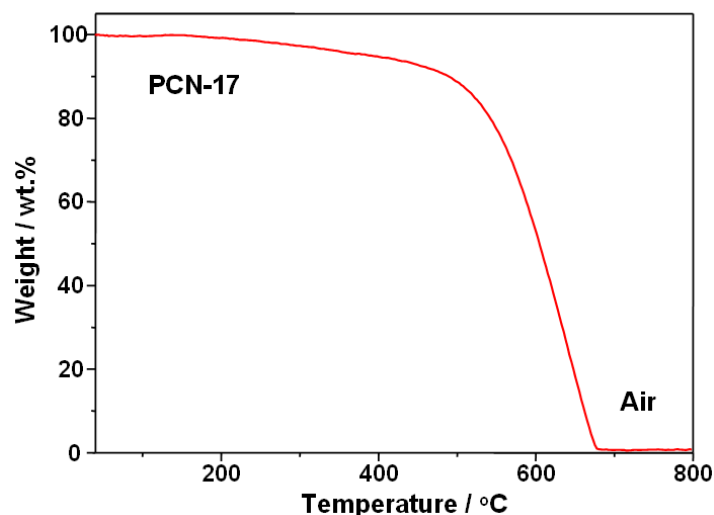


**Fig. S6** Thermogravimetric (TG) analysis of PCN-17 under air. The thermal stability of the products was evaluated using a thermal analyzer (Netzsch STA 449 F3) from 40 to 800 °C under air with a heating rate of 10 °C/min.

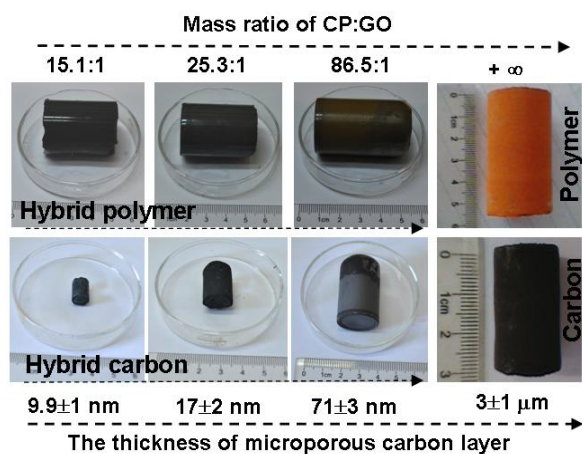


**Fig. S7** Optical photographs of the obtained polymers and carbons under different CP/GO mass ratios. The control sample prepared without using GO was shown on the right side.

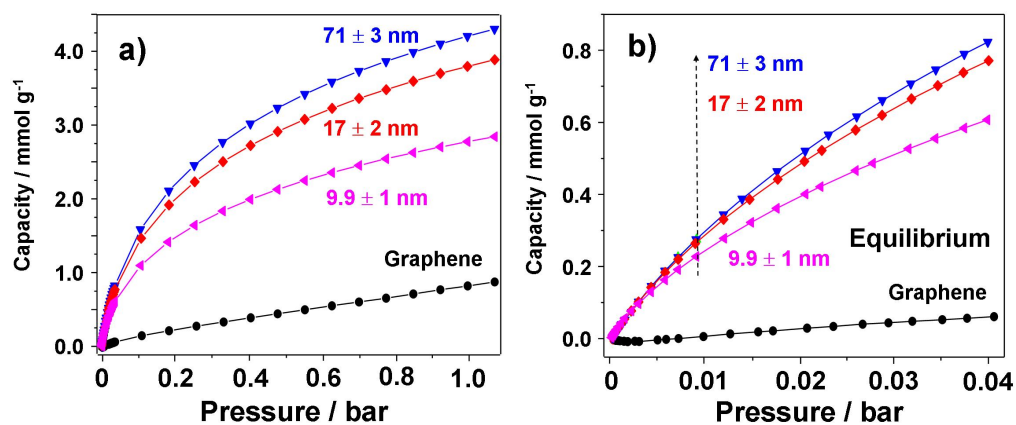


**Fig. S8** a) CO<sub>2</sub> adsorption isotherms at 0 °C; b) low pressure range CO<sub>2</sub> adsorption isotherms at 0 °C where the solid line represents a Toth model fit to the CO<sub>2</sub> isotherms.

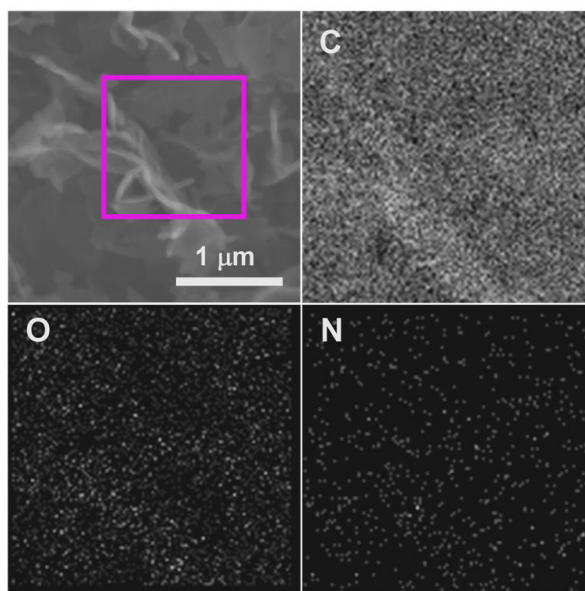


**Fig. S9** The EDX mapping images of C, O and N elements for sample PCN-17. It shows the uniform distribution of N elements, indicating the N-doped feature of this sample.



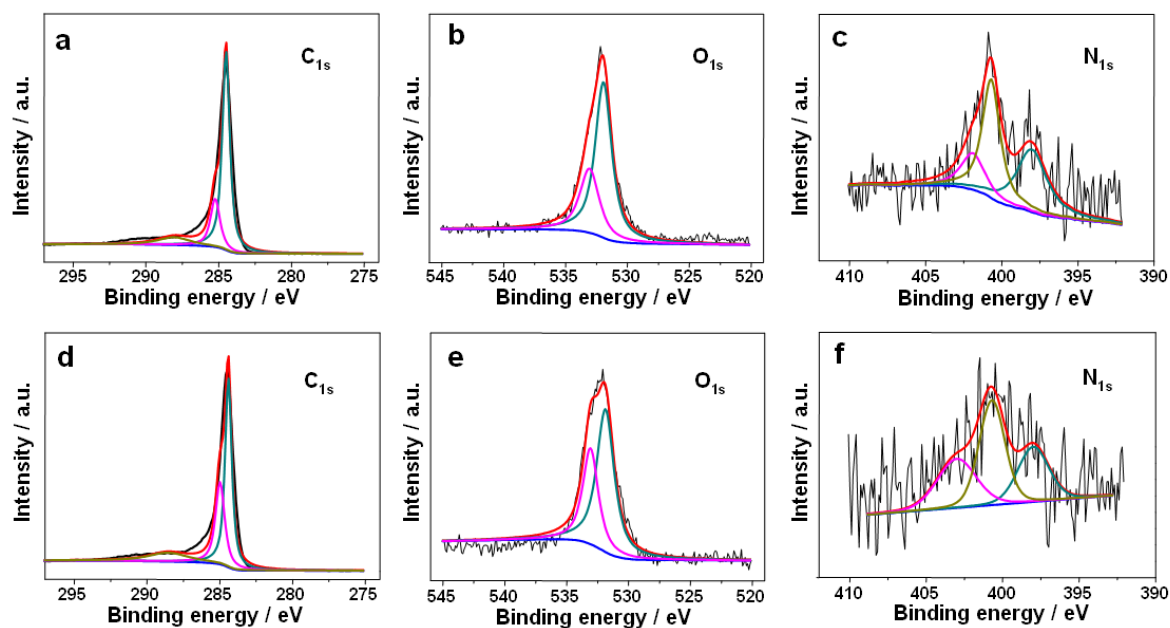


**Fig. S10** C<sub>1s</sub>, O<sub>1s</sub>, and N<sub>1s</sub> XPS spectra of PCN-17 a, b, and c) and PCN-71 d, e, and f). X-ray photoelectron spectroscopy (XPS) measurements were performed using a Thermo VG Scientific ESCALAB 250Xi spectrometer with Al K $\alpha$  radiation (1486.6 eV). Binding energies were corrected for surface charging by referencing them to the energy of the C1s peak of the contaminant carbon at 284.6 eV.

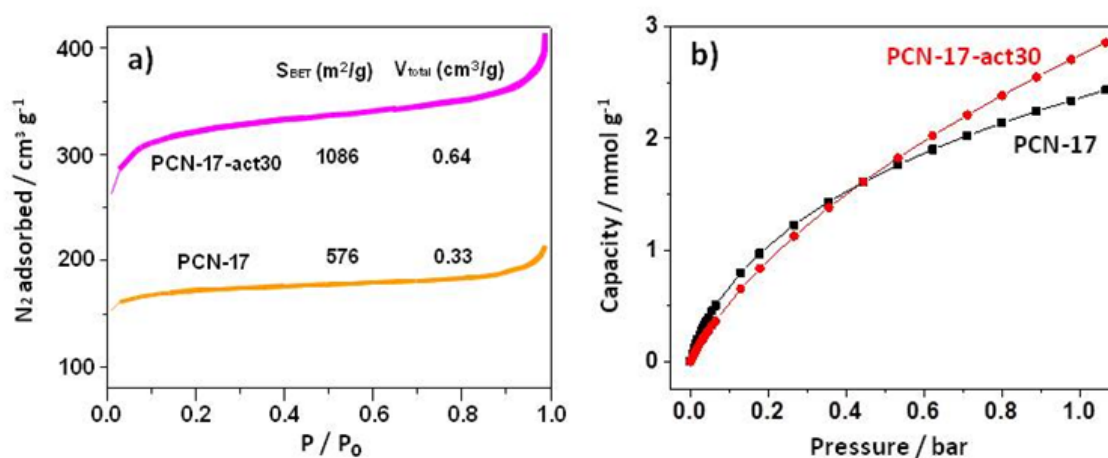


**Fig. S11** a) The N<sub>2</sub> sorption isotherms for sample of PCN-17 before and after steam activation. b) CO<sub>2</sub> adsorption isotherms for sample of PCN-17 before and after steam activation under high and low CO<sub>2</sub> partial pressures at 25 °C, where the solid line represents a Toth model fit to the CO<sub>2</sub> isotherms.



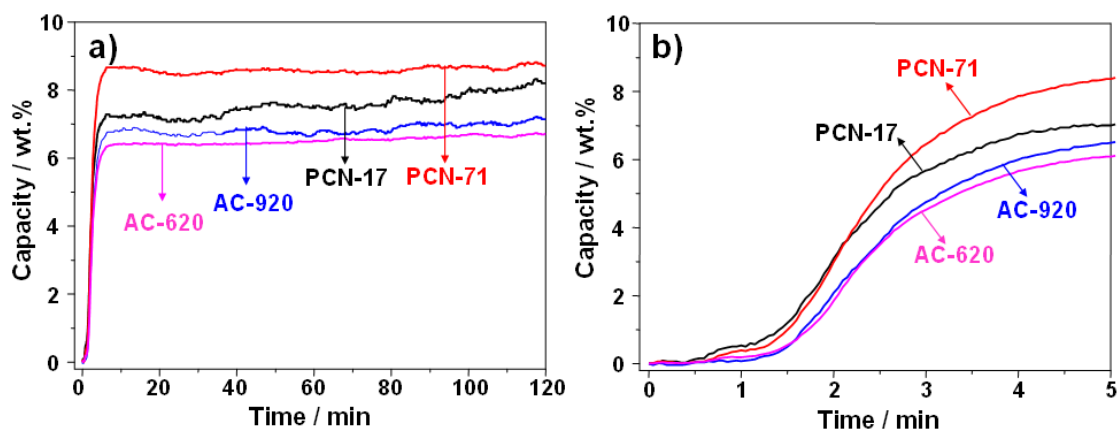


**Fig. S12** Time-resolved CO<sub>2</sub> adsorption of PCN-17, PCN-71 and reference activated carbon (AC-920 and AC-620, surface area: 920 m<sup>2</sup> g<sup>-1</sup> and 620 m<sup>2</sup> g<sup>-1</sup>) at 25 °C. This time-resolved CO<sub>2</sub> sorption curves were obtained using a thermal analyzer (Netzsch STA 449 F3) based on gravimetric methods.

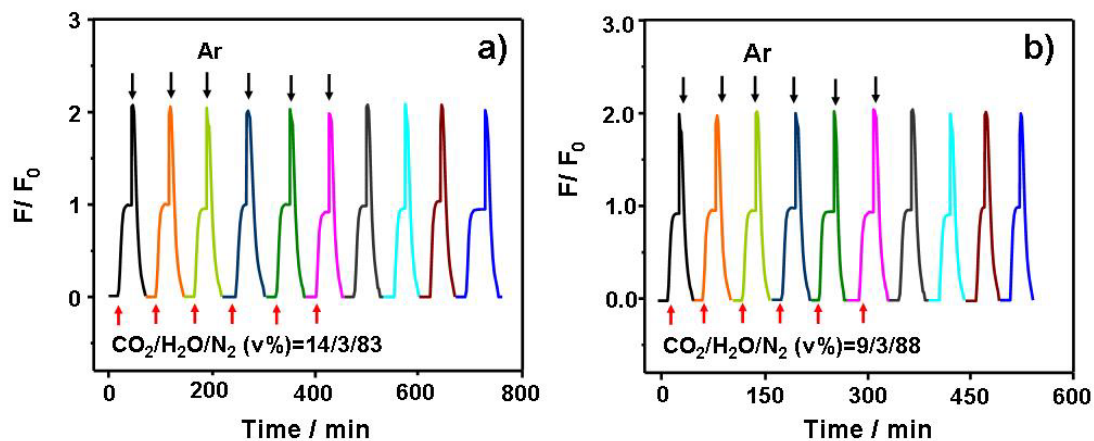


**Fig. S13** Regeneration cycles of CO<sub>2</sub> separation of PCN-17 from a stream of CO<sub>2</sub>/H<sub>2</sub>O/N<sub>2</sub> of 14/3/83 and 9/3/88 v% at 25 °C, followed regeneration by Ar purge at 50 °C.

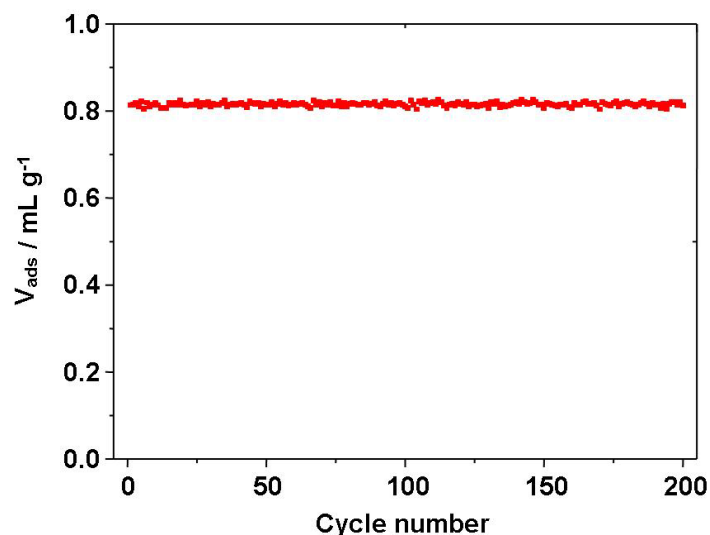


**Fig. S14** A dynamical 200-cycles of CO<sub>2</sub> separation of PCN-17 from a stream of CO<sub>2</sub>/N<sub>2</sub> of 14/86 at 25 °C, followed regeneration by Ar purge at 50 °C.

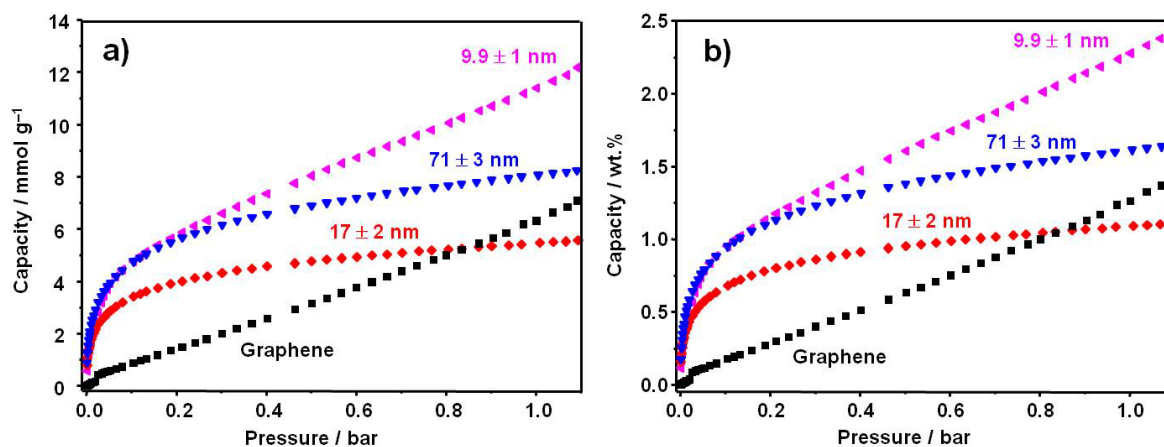


**Fig. S15** Hydrogen adsorption isotherms of the PCNs: a) mole capacity, b) weight capacity. The H<sub>2</sub> sorption isotherms of the PCNs were measured using a Micromeritics ASAP 2020 static volumetric analyzer at 77 K and 1 bar.

## References

- 1 B. Wang, A. P. Côté, H. Furukawa, M. O’Keeffe and O. M. Yaghi, *Nature* 2008, **453**, 207–211.
- 2 A. Malek and S. Farooq, *AIChE Journal* 1996, **42**, 3191–3201.
- 3 S. Himeno, T. Komatsu and S. Fujita, *J. Chem. Eng. Data* 2005, **50**, 369–376.
- 4 M. M. Maroto-Valer, Z. Tang and Y. Z. Zhang, *Fuel Process. Technol.* 2005, **86**, 1487–1502.
- 5 C. Pevida, M. G. Plaza, B. Arias, J. Feroso, F. Rubiera and J. J. Pis, *Appl. Surf. Sci.* 2008, **254**, 7165–7172.
- 6 Z. J. Zhang, M. Y. Xu, H. H. Wang and Z. Li, *Chem. Eng. J.* 2010, **160**, 571–577.
- 7 T. C. Drage, A. Arenillas, K. M. Smith, C. Pevida, S. Piippo and C. E. Snape, *Fuel* 2007, **86**, 22–31.

- 8 L. Y. Meng and S. J. Park, *J. Colloid Interface Sci.* 2010, **352**, 498–503.
- 9 Z. Zhang, J. Zhou, W. Xing, Q. Xue, Z. Yan, S. Zhuo and S. Z. Qiao, *Phys. Chem. Chem. Phys.* 2013, **15**, 2523–2529.
- 10 M. Sevilla and A. B. Fuertes, *J. Colloid Interface Sci.* 2012, **366**, 147–154.
- 11 D. Saha and S. Deng, *J. Colloid Interface Sci.* 2010, **345**, 402–409.
- 12 G. Chandrasekar, W.-J. Son and W.-S. Ahn, *J Porous Mater.* 2009, **16**, 545–551.
- 13 G.-P. Hao, W.-C. Li, D. Qian and A.-H. Lu, *Adv. Mater.* 2010, **22**, 853–857.
- 14 G.-P. Hao, W.-C. Li, D. Qian, G.-H. Wang, W.-P. Zhang, T. Zhang, A.-Q. Wang, F. Schüth, H.-J. Bongard and A.-H. Lu, *J. Am. Chem. Soc.* 2011, **133**, 11378–11388.
- 15 Y. Zhu, S. Murali, M. Stoller, K. J. Ganesh, W. Cai, P. J. Ferreira, A. Pirkle, R. M. Wallace, K. A. Cychoz, M. Thommes, D. Su, E. A. Stach, R. S. Ruoff, *Science* 2011, **332**, 1537-1541.
- 16 B. Wang, A. P. Côté, H. Furukawa, M. O’Keeffe and O. M. Yaghi, *Nature* 2008, **453**, 207–211.
- 17 R. Banerjee, H. Furukawa, D. Britt, C. Knobler, M. O’Keeffe and O. M. Yaghi, *J. Am. Chem. Soc.* 2009, **131**, 3875–3877.
- 18 Q. Lin, T. Wu, S.-T. Zheng, X. Bu and P. Feng, *J. Am. Chem. Soc.* 2012, **134**, 784–787.
- 19 J. An, S. J. Geib and N. L. Rosi, *J. Am. Chem. Soc.* 2010, **132**, 38–39.